Time-Resolved Absorption and Photothermal Measurements with Sensory Rhodopsin I from *Halobacterium salinarum*

Aba Losi,* Silvia E. Braslavsky,* Wolfgang Gärtner,* and John L. Spudich#
*Max-Planck-Institut für Strahlenchemie, Postfach 101365, D-45413 Mülheim an der Ruhr, Germany and #Department of Microbiology and Molecular Genetics, University of Texas Medical School, 1.708 JFB, 6431 Fannin, Houston, Texas 77030

ABSTRACT An expansion accompanying the formation of the first intermediate in the photocycle of transducer-free sensory rhodopsin I (SRI) was determined by means of time-resolved laser-induced optoacoustic spectroscopy. For the native protein (SRI-WT), the absolute value of the expansion is ~5.5 mL and for the mutant SRI-D76N, ~1.5 mL per mol of phototransformed species (in 0.5 M NaCl), calculated by using the formation quantum yield for the first intermediate (S_{610}) of Φ_{610} = 0.4 ± 0.05 for SRI-WT and 0.5 ± 0.05 for SRI-D76N, measured by laser-induced optoacoustic spectroscopy and by laser flash photolysis. The similarity in Φ_{610} and in the determined value of the energy level of S_{610}, E_{610} = (142 ± 12) kJ/mol for SRI-WT and SRI-D76N indicates that Asp^{76} is not directly involved in the first step of the phototransformation. The increase with pH of the magnitude of the structural volume change for the formation of S_{610} in SRI-WT and in SRI-D76N upon excitation with 580 nm indicates also that amino acids other than Asp^{76}, and other than those related to the Schiff base, are involved in the process. The difference in structural volume changes as well as differences in the activation parameters for the S_{610} decay should be attributed to differences in the rigidity of the cavity surrounding the chromophore. Except for the decay of the first intermediate, which is faster than in the SRI-transducer complex, the rate constants of the photocycle for transducer-free SRI in detergent suspension are strongly retarded with respect to wild-type membranes (this comparison should be done with great care because the preparation of both samples is very different).

INTRODUCTION

Sensory rhodopsin I (SRI), a phototaxis receptor in *Halobacterium salinarum,* is a member of the retinal-containing, membrane-intrinsic protein family of Archaea (Hoff et al., 1997). Photoexcitation of SRI (λ_{max} = 587 nm) causes isomerization of the retinal chromophore and converts the parent state into a UV-absorbing signaling state (S_{373}) containing a deprotonated Schiff-base (Haupts et al., 1994). In vivo, SRI is physically coupled to a methyl-accepting transducer protein, *Htr*I, that modulates cell motility (Yao and Spudich, 1992).

The first step in the SRI photocycle is the formation of the red-shifted S_{610} intermediate in the subnanosecond timescale (Bogomolni and Spudich, 1987), following the all-*trans* to 13-*cis* photoisomerization of retinal. In SRI-*Htr*I complexes, the subsequent intermediate (S_{560}) is formed in 90 μs and decays to S_{373} with a lifetime of 270 μs. The destiny of S_{373} is to thermally decay to the parent state with a 750 ms lifetime. If irradiated with near-UV light, S_{373} transforms into S_{510}, which then decays to the parent state with a lifetime of 80 ms (Spudich and Bogomolni, 1984).

In the cell, the orange light excitation of SRI and near UV photoreaction of S_{373}, generate attractant and repellent responses, respectively (for a recent review see Hoff et al., 1997). Removal of the transducer dramatically affects the kinetics of the photocycle: the decay of S_{373} becomes pH dependent (Spudich and Spudich, 1993) and the time constants for the rise and the decay of this intermediate are significantly changed (Olson and Spudich, 1993; Haupts et al., 1996). Removal of the transducer not only changes the photocycle kinetics but also renders SRI into a pH-dependent proton pump (Bogomolni et al., 1994; Haupts et al., 1996).

A major question for the understanding of the mechanism of light-to-signal transduction in chromoproteins is the chromophore–protein interaction along the photocycle. In this context, the knowledge of the quantum yields, lifetimes, structural volume changes, and energy content of intermediates in wild type protein as well as in mutated SRI is of fundamental importance. In SRI the Asp^{76} residue corresponds to the proton acceptor Asp^{85} in bacteriorhodopsin (BR) (Butt et al., 1989) and plays the same role when SRI acts as a proton pump. A mutation in this residue is thus expected to affect the photochemical properties and the function of the protein (see below).

We report, in this paper, on the results of the study of the transducer-free, detergent-solubilized SRI as well as of the mutated detergent-solubilized SRI-D76N photocycle by means of laser-induced optoacoustic spectroscopy (LIOAS) and flash photolysis with optical detection. As a first step in our studies with these proteins, detergent-solubilized samples were chosen because of the low scattering of the samples.

LIOAS is a time-resolved photocalorimetric technique that measures enthalpy and structural volume changes in photoinitiated reactions (Braslavsky and Heibel, 1992). In addition to being used for studies on model compounds,

Received for publication 27 October 1998 and in final form 6 January 1999.

Address reprint requests to Dr. Silvia E. Braslavsky, Max-Planck-Institut für Strahlenchemie, Postfach 101365, D-45413 Mülheim an der Ruhr. Fax: +49(208)306-3681; E-mail: braslavskys@mpi-muelheim-mpg.de.

0006-3495/99/04/2183/09 $2.00

LIOAS has been used for photocalorimetric studies on biological photoreceptors (for a review, see Schulenberg and Braslavsky, 1997). As long as the time constants of the photoinduced processes fall within the integration time of the method (15 ns to ~5 μs), deconvolution techniques yield the time constants of these reactions (Rudzki-Small et al., 1992) allowing the correlation of the various steps with those determined by time-resolved optical techniques.

The rationale behind the LIOAS measurements is that, after pulse excitation of a light-absorbing solution, a volume change occurs due to heat release by radiationless processes and to structural volume changes (intrinsic and caused by solvent rearrangements). In aqueous solutions, the separation of both contributions to the LIOAS signal is readily achieved by performing the experiments at various temperatures in a relative small temperature range, taking advantage of the fact that the thermoelastic parameters of water strongly depend on temperature. If enough complementary information is available on the photophysics of the system, it is possible to determine formation quantum yields (Φ_i) and structural volume changes ($\Delta V_{R,i}$) associated with the *i*th photoreaction (Braslavsky and Heibel, 1992; Gensch et al., 1998).

MATERIALS AND METHODS

His-tagged, transducer-free wild type SRI-WT and the D76N mutant were prepared as already described (Krebs et al., 1995; Rath et al., 1996). In the protocol, membranes prepared from low salt dialysis of cells are extracted with 1.0% w/v lauryl maltoside and the solubilized his-tagged receptors purified by Ni^{2+}-affinity chromatography. The final solutions contained 0.025% lauryl maltoside, 4 M NaCl, and 50 mM MES, pH 6, and were diluted to NaCl concentrations of 0.25 or 0.5 M for the LIOAS and flash photolysis experiments. Bromocresol green, Evans blue, and lauryl (*n*-dodecyl-β-D)-maltoside were from Sigma Chemical Co. (St. Louis, MO). The pH of the solutions was adjusted by the addition of a concentrated NaOH solution. Bacteriorhodopsin used as an actinometric reference was prepared according to (Oesterhelt and Stoeckenius, 1997).

Absorption spectra were recorded with a Shimadzu UV-2102PC spectrophotometer. For the LIOAS experiments reference and sample absorbances were matched within 5% at the excitation wavelength. Excitation was with the 11-ns pulses from a Nd:YAG laser (Spectron Laser Systems SL802, Rugby, UK)-pumped dye laser (Spectron Laser Systems SL4000G) using Rhodamine B for 580 nm, as described previously (Malkin et al., 1994; Gensch and Braslavsky, 1997). The beam was shaped by a slit (0.5 × 6 mm), which determines an acoustic transit time in aqueous solution of about 300 ns, allowing time resolution down to ~30 ns by using deconvolution techniques (Rudzki et al., 1985). The pulse fluence was varied with a neutral density filter and measured with a pyroelectric energy meter (RJP735 head connected to a meter RJ7620 from Laser Precision Corp.). The signal was detected by a Pb-Zr-Ti ceramic piezoelectric transducer (PZT, 4 mm, Vernitron), amplified (100 times, Comlinear E103, Loveland, CO), digitized by a digital oscilloscope (Tektronik TDS 684A, Beaverton, OR, operating at 500 megasample/s), and stored in a VAX station 3100 and a personal computer for further treatment of the data. Normally, 40 signals were averaged for the sample and 100 for the reference. Given the slow photocycle of the proteins, the pulse frequency was kept very low (around 0.3 Hz); no changes in the time profile or amplitude of the signals were observed up to 0.5 Hz for SRI-D76N and up to 1 Hz for SRI-WT. Care was taken to perform the experiments in the linear regime of amplitude versus laser fluence, which was up to 30 μJ per pulse. The incident fluence actually used was between 15 and 20 μJ per pulse.

Deconvolution of the LIOAS waveform was performed by means of an iterative least-squares algorithm. The time evolution of the pressure was assumed to be a sum of single exponential functions. The analysis yielded the fractional amplitudes (φ_i) and the lifetimes (τ_i) of the transients (Sound Analysis 3000, Quantum Northwest Inc., Spokane, WA). The time window was between 20 ns and 5 μs; decays faster than 10 ns were integrated by the transducer, whereas decays longer than 5 μs were not sensed.

The thermoelastic parameters of the buffers were determined by comparison with those of pure water, following the methodology described in Borsarelli and Braslavsky (1997) and Churio et al. (1994). The identity of the isothermal compressibility and the adiabatic compressibility in water was assumed to hold in the buffer solution. Evans blue and bromocresol green were used as calorimetric reference compounds in neat water and in the buffer solutions, respectively.

Flash photolysis measurements were performed with an apparatus already described by Ruddat et al. (1997). The samples were measured in a 1-cm pathlength cuvette, and the sample concentration was ~5 μM, which meant an absorbance ~0.25 at 580 nm. The excitation was with the same laser as used for the LIOAS experiments (see above). Fluence and polarization were controlled by optical elements and the pulse was shaped to a circular spot of 2.5 cm diameter. The analyzing light (perpendicular to the excitation beam) was delivered by a 100-W continuous wave tungsten halogen lamp for detection in the millisecond-to-second range and a 150-W pulsed xenon arc for microsecond detection. Transient absorption measurements were performed under magic angle conditions to avoid artifacts caused by rotational diffusion. Filters, a shutter, and a monochromator in front of the sample reduced analyzing light intensity and exposure time to suppress secondary photochemistry. A dual-beam detection arrangement compensated fluctuations in the analyzing beam intensity. Photomultiplier tubes (Hamamatsu R3896, Herrsching, Germany) served as detectors in the observation and reference pathways; a second monochromator was placed in front of the photomultiplier, whereas the reference pathway included only filters. The photocurrents of the photomultipliers were coupled to ground through resistors of variable values, depending on the analyzed time window. The voltages were recorded with a transient digital oscilloscope (Tektronix TDS 520a) and transferred to a VAX station and a personal IBM computer for data analysis.

Fitting of the kinetics traces was performed with a sum of single-exponential kinetic functions using the program Origin 4.1 (Microcal Software Inc., Northampton, MA).

LIOAS data handling and modeling

The amplitudes (φ_i) recovered from deconvolution, are related to the heat released (q_i) and structural volume changes ($\Delta V_{r,i}$) by (Rudzki et al., 1985; Rudzki-Small et al., 1992)

$$E_\lambda \varphi_i = q_i + \Delta V_{r,i} \frac{c_p \rho}{\beta}, \qquad (1)$$

where E_λ is the molar excitation energy, $\beta = (\partial V/\partial T)_p\, 1/V$ is the volume expansion coefficient, c_p is the heat capacity at constant pressure, and ρ is the mass density of the solvent. Thus, $c_p\rho/\beta$ is the ratio of thermoelastic parameters. $\Delta V_{r,i} = \Phi_i \Delta V_{R,i}$, where Φ_i is quantum yield of the *i*th process, and $\Delta V_{R,i}$ is the structural volume change per mol of phototransformed species. The values of q_i and $\Delta V_{r,i}$ were derived either by the several-temperature (ST) or by the two-temperature (TT) method. For a comparison between the two methods, see Gensch and Braslavsky (1997) and Losi and Viappiani (1998). When the ST method is applied, q_i is recovered from the intercept and $\Delta V_{r,i}$ from the slope of $E_\lambda\varphi_i$ versus $c_p\rho/\beta$ plots, provided that both parameters remain constant over the relatively small temperature range used to achieve a significant variation in $c_p\rho/\beta$. The fraction of absorbed energy released as heat in the *i*th step is $\alpha_{thi} = q_i/E_\lambda$. When using the TT method, the sample waveform was acquired at the temperature for which $\beta = 0$ ($T_{\beta=0}$) and sample and reference solutions were also measured

at a slightly higher temperature $T_{\beta>0}$. In this case (Malkin et al., 1994),

$$\Delta V_{r,i} = E_\lambda \varphi_i \left(\frac{\beta}{c_p \rho}\right)_{T_{\beta>0}}. \quad (2)$$

From simple energy balance considerations, the prompt heat release (α_{th1}) for all processes with lifetime $\tau_{pr} < 10$ ns (corresponding to the formation of S_{610}) is expressed by

$$\alpha_{th1} = 1 - \Phi_F \frac{E_F}{E_\lambda} - \Phi_{S610} \frac{E_{S610}}{E_\lambda}. \quad (3)$$

The quantum yield of fluorescence is negligible ($\Phi_F < 0.02$) and the 0–0 energy (187 kJ/mol) is taken as an upper limit for E_{S610}, in view of the fact that the subsequent steps after S_{610} are all exothermic. Thus, a lower limit for Φ_{S610} is given by

$$\Phi_{S610} \geq (1 - \alpha_{th1}) \frac{E_\lambda}{E_{0-0}}. \quad (4)$$

For SRI-D76N, the decay of S_{610} is short enough to be detectable by LIOAS (see Results). Thus, it is possible to formulate Eq. 5, which describes the heat evolved during the second step of the photoinduced cycle as a function of the quantum yields for the formation of each species and their respective energy levels, as long as the two processes are well separated in time and no equilibrium between transients is involved.

$$\alpha_{th2} = \Phi_{S610} \frac{E_{S610}}{E_\lambda} - \Phi_{S560} \frac{E_{S560}}{E_\lambda}. \quad (5)$$

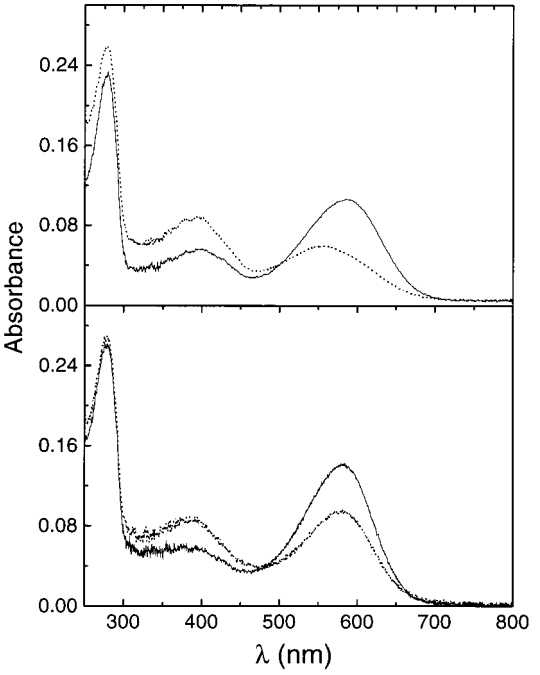

FIGURE 1 Absorption spectra of SRI-WT (*top*) and SRI-D76N (*bottom*). *Straight lines,* pH 6.0; *dotted lines,* pH 7 for SRI-WT and 7.2 for SRI-D76N. Sample conditions: 50 mM MES, 0.025% lauryl-maltoside, 0.5 M NaCl.

RESULTS

Absorption spectra

The absorption spectra of SRI-WT and of SRI-D76N at two different pH values are shown in Fig. 1. At pH 7, the Schiff base is partially deprotonated in both proteins as indicated by the increased absorption at 390 nm with respect to that at pH 6. In SRI-WT, the deprotonation of Asp^{76} becomes obvious from the blue shift of the main absorption band from 580 to 550 nm upon increasing the pH from 6.0 to 7.0 (Krebs et al., 1995).

Flash photolysis

S_{610} was monitored at 680 nm to avoid overlapping of spectra as much as possible. The decay of this transient (Fig. 2, *top*), is much faster both for SRI-WT and for the mutant SRI-D76N than in the transducer-coupled protein, which was determined as 90 μs at ambient temperature (Bogomolni and Spudich, 1987). At 6°C, the lifetime of S_{610} was 10 μs for SRI-WT (Fig. 2, *left series*) and 3.6 μs for SRI-D76N (Fig. 2, *right series*).

For both samples, the decay of this species (τ_1 in Table 1) was strongly temperature dependent (Fig. 3). The parameters obtained upon application of the Arrhenius and the Eyring equations are reported in Table 2.

The formation of S_{373}, monitored at 380 nm (Fig. 1), is biexponential (τ_3 and τ_4, Table 1), whereas its decay is in a single step and concomitant with the recovery of the parent state as monitored at 580 nm for SRI-WT and at 570 nm for SRI-D76N.

The S_{610} formation quantum yield (Φ_{610}) was determined by using the comparative method in flash photolysis (Bensasson et al., 1978). Bacteriorhodopsin was used as an actinometer. The formation of the M intermediate of BR ($\Phi_M = 0.64$) was monitored 1 ms after the pulse at 602 nm ($\epsilon_{BR602} = 43{,}000\ M^{-1}\ cm^{-1}$) (Tittor and Oesterhelt, 1990). The absorption changes after excitation of SRI were measured at 680 nm 1 μs after the laser pulse (ΔA_{680}). A molar absorption coefficient for S_{610} at 680 nm of $\epsilon_{S610} \approx 16{,}000\ M^{-1}\ cm^{-1}$ was used. This value was derived from the data reported by Bogomolni and Spudich (1987). The linear part of the plots ΔA_λ versus laser fluence (E_{exc}) was used for both BR and SRI, by applying Eq. 6, following the methodology described by van Brederode et al. (1995),

$$\Phi_{610} = \Phi_M \frac{(\Delta A^{SRI}_{680}/E_{exc})}{(\Delta A^{BR}_{602}/E_{exc})} \frac{\epsilon^{BR}_{602}}{\epsilon^{S610}_{680}}. \quad (6)$$

The $\Delta A^i_\lambda/E_{exc}$ are the slopes of the corresponding linear plots of the fluence (E_{exc})-dependent transient absorbances after the laser pulse. It was assumed that the only two species present 1 μs after the excitation are S_{610} and the parent state of SRI. To obtain the absorbance change due only to the rising of S_{610}, a correction factor was applied, according to the equation

$$\Delta A^{S610}_{680} = \frac{\Delta A^{SRI}_{680}}{1 - \epsilon^{SRI}_{680}/\epsilon^{S610}_{680}}.$$

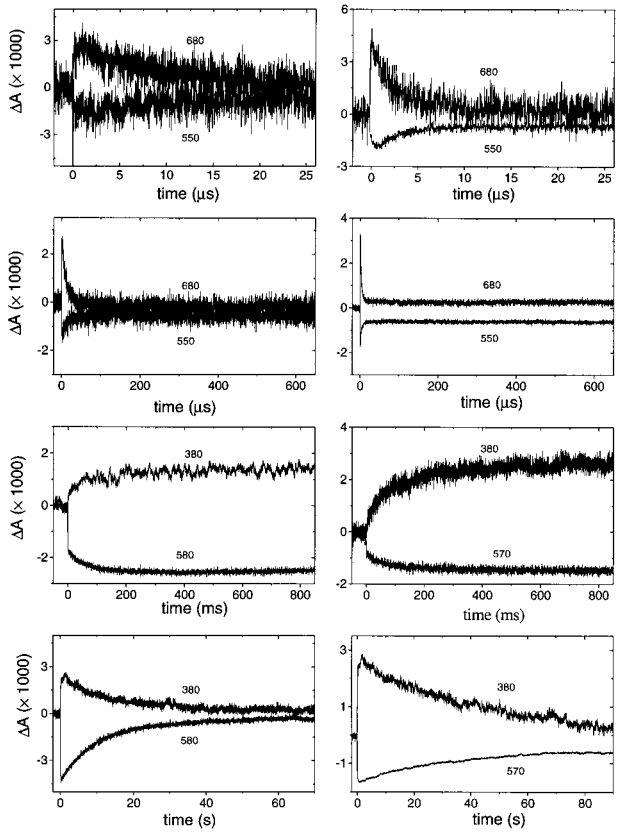

FIGURE 2 Transient absorption decay traces in the time range from microseconds to seconds for SRI-WT (*left*) and SRI-D76N (*right*). λ_{exc} = 580 nm; the wavelength of the probe beam is indicated in each plot. The concentration of the samples was around 4 μM, $A_{580} \approx 0.2$, $T = 6$°C. The sample conditions were as in Fig. 1.

The correction factor in the denominator of the right term is 0.9 for SRI-D76N and 0.76 for SRI-WT.

The values obtained for the quantum yields of S_{610} production were $\Phi_{S610} = 0.4 \pm 0.05$ for SRI-WT and 0.5 ± 0.05 for SRI-D76N. The errors reported (standard deviations) arise from the averaging of 3 independent sets of measurements, but it should be noted that other sources of error (e.g., the true absorbance in scattering samples and the values of the transient absorption coefficients) may contribute to the uncertainty in Φ_{S610}.

TABLE 1 Transient lifetimes after excitation of SRI-WT and SRI-D76N, as derived from multiexponential fitting of the kinetics curves at 6°C, from the flash photolysis experiments (Figure 2)

	τ_1 (μs)	τ_2 (ms)	τ_3 (ms)	τ_4 (ms)	τ_5 (s)
SRI-WT	10.2 ± 0.4	—	57 ± 2	296 ± 20	11.7 ± 0.2
SRI-D76N	3.7 ± 0.1	3 ± 0.9	30 ± 3	178 ± 11	28.3 ± 0.2

τ_1 corresponds to the S_{610} decay and S_{560} rise, τ_3 and τ_4 to the biexponential S_{373} rise, τ_5 to the S_{373} decay and parent state recovery. τ_2 has not been assigned, it is detected for SRI-D76N at 680 (decay) and at 550 nm (rise).

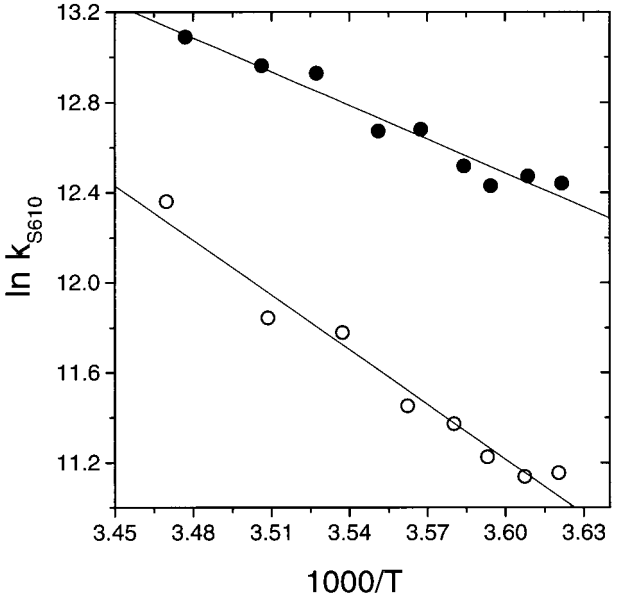

FIGURE 3 Arrhenius plots for the decay of S_{610} as derived from flash photolysis data. Sample conditions were as in Fig. 1. λ_{exc} = 580 nm, λ_{obs} = 680 nm. T range = 3–15°C; τ_{610} range: 2–4 μs for SRI-D76N (*filled symbols*) and 4.5–14.5 μs for SRI-WT (*open symbols*). See Table 2 for fitting of the results.

LIOAS results

For both proteins, plots of φ_1 versus $c_p\rho/\beta$ yielded a positive slope, indicating that the SRI $\rightarrow S_{610}$ step (associated with τ_{pr}) is accompanied by an expansion (Eq. 1, Fig. 4 for SRI-WT).

The signal recorded at $T_{\beta=0}$ (0 and −3.5°C for [NaCl] = 0.25 and 0.5 M, respectively) confirms the occurrence of the expansion. Results obtained at pH = 6 with the ST and TT methods are reported in Table 3 along with $\Delta V_{R,1}$ and the lower limit for Φ_{610} (Eq. 4). The differences between the two methods fall generally within the experimental error. For SRI-WT, the production of S_{610} was the only detectable step. For SRI-D76N at $T > 10$°C, in addition to $\tau_{pr} < 10$ ns, a second transient of amplitude φ_2 was retrieved by deconvolution (Fig. 5). The amplitudes associated with this transient were very small. This, together with the poor resolution of LIOAS in the microsecond region, may explain

TABLE 2 Activation parameters for the decay of S_{610} in SRI

pH = 6, T = 3–15°C	SRI-WT	SRI-D76N
A (s^{-1})	(3 ± 0.1) 10^{17}	(1.6 ± 0.3) 10^{13}
E_a (kJ/mol)	67 ± 5	41 ± 4
$\Delta S^{\#}$ (J/mol K)	83 ± 18	0 ± 3
$\Delta H^{\#}$ (kJ/mol)	65 ± 5	39 ± 4

The preexponential factor, A, and the activation energy, E_a are derived from the Arrhenius plots depicted in Figure 3 ($\ln k = \ln A - E_a/RT$) whereas the activation entropy ($\Delta S^{\#}$) and enthalpy ($\Delta H^{\#}$) are derived from the Eyring fitting, i.e., $\ln(k/T) = \ln(k_B/h) + \Delta S^{\#}/R - \Delta H^{\#}/RT$ (k_B and h are Boltzmann and Planck constant, respectively).

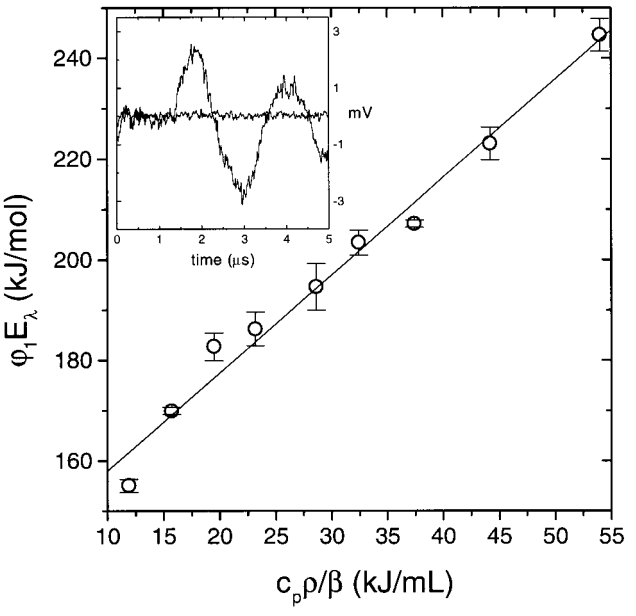

FIGURE 4 Plot of $\varphi_1 E_\lambda$ versus the ratio of thermoelastic parameters for SRI-WT (Eq. 1). λ_{exc} = 580 nm. Sample conditions were as in Fig. 1, except for [NaCl] = 0.25 M. *Inset:* LIOAS signal for the protein at $T_{\beta=0}$ = 0°C.

the difficulties in retrieving the decay of S_{610} at lower temperatures.

The lifetimes associated with the decay of S_{610} (τ_{610} = 1.2 μs at 18°C) obtained by LIOAS for the mutant SRI-D76N, are close to the values of τ_1 (Table 1) obtained by fitting the kinetics traces for the decay of ΔA_{680} from flash photolysis at the same temperature (1.4 μs at 18°C).

The plots of φ_2 versus $c_p\rho/\beta$ had again a positive slope, indicating that the decay $S_{610} \rightarrow S_{560}$ is also accompanied by an expansion. The corresponding α_{th2} was close to zero, i.e., the enthalpy change associated with this decay should be very small (see Table 3).

In an attempt to elucidate the origin of the structural volume changes, we investigated the influence of pH, which affects the protonation state of the Schiff base and of Asp^{76} (Krebs et al., 1995; Rath et al., 1996). The LIOAS parameters obtained at pH 6 and pH 7 (7.2 for D76N) upon 532 nm excitation are summarized in Table 4. For both proteins, α_{th1} remained the same at the two pH values, whereas $\Delta V_{R,1}$ increased. As expected, Φ_{610} was the same, within the experimental error, as for 580 nm excitation (Table 3).

Titration of the parent states

For both proteins, the titration curves up to pH 7.5 are consistent with the involvement of only one proton. $\Delta V_{R,1}$ increased quite monotonically with pH (Fig. 6, *bottom*). For SRI-WT, we obtained about the same pK_a value from absorption data (6.4 ± 0.1, Fig. 6 *top, open circles*) as from a plot of $\Delta V_{R,1}$ versus pH (pK_a around 6.5, Fig. 6 *bottom, open circles*). This value agrees with that reported for the pK_a value of the Schiff base and of Asp^{76} [pK_a = 6.5, (Krebs et al., 1995)]. For SRI-D76N, the pK_a = 6.9, corresponding only to the Schiff base protonation, is slightly larger.

For SRI-D76N, we obtained a value of pK_a = 6.9 ± 0.1 from the absorption data (Fig. 6 *top, filled circles*), smaller than the value previously reported for the deprotonation of the Schiff base in a 4-M NaCl solution [pK_a = 7.6, (Rath et al., 1996)]. The difference is probably due to the different salt concentration used (Fig. 6). For pH ≥ 8.2, the absorption at the excitation wavelength was too low to yield good LIOAS signals. A tentative fitting of the data between pH 6 and 7.6, afforded a value of pK_a = 6.9 (Fig. 6 *bottom, filled circles*). Even though this value agrees with the one from absorption data, plots of $\Delta V_{R,1}$ versus pH were very steep and not consistent with a monoprotic equilibrium. The reason for this behavior should be that the structural volume change is determined by amino acids other than those involved in the formation of the Schiff base.

DISCUSSION

For both the WT protein and the D76N mutant, the formation of S_{610} in the transducer-free system and in the presence of detergent at pH 6 was accompanied by a relatively small expansion of ~5.5 mL (WT) and ~1.5 mL (mutant) per mole of produced transient ($\Delta V_{R,1}$ in Tables 3 and 4). A similar expansion of 5 mL/mol has been found also in bovine rhodopsin for the first step, i.e., the formation of bathorhodopsin (Strassburger et al., 1997). For the formation of the K intermediate in bacteriorhodopsin, Schulenberg et al. (1994) reported a small contraction of 11 mL/mol of phototransformed species, whereas Zhang and Mauzerall (1996) reported a small expansion of 1.5 mL/mol. The reason for this discrepancy remains to be clarified.

The fraction of energy released as heat in the first step (α_{th1} minus the vibrational relaxation term within the excited singlet manifold), i.e., upon formation of S_{610} (associated with $\tau_{pr} < 10$ ns), is calculated with Eq. 7 (a simple modification of Eq. 3) to be 56% and 53% after 580 and 532 nm excitation, respectively, for SRI-D76N and 60% after excitation with both wavelengths for SRI-WT. The expected variation of released energy upon variation of the excitation wavelength, as observed for the mutant, apparently is too small to be detected in the case of the WT protein.

$$\alpha_{th1} - \frac{E_\lambda - E_{0-0}}{E_\lambda} = (1 - \Phi_{S610})\frac{E_{0-0}}{E_\lambda} + \Phi_{S610}\frac{(E_{0-0} - E_{S610})}{E_\lambda}. \quad (7)$$

By using the values of quantum efficiency, Φ_{S610} = 0.5 for SRI-WT and 0.4 for SRI-D76N, as derived from transient absorption data after flash photolysis, an average of E_{S610} = (142 ± 12) kJ/mol for SRI-WT, i.e., a 45 kJ/mol

TABLE 3 LIOAS data for SRI-WT and SRI-D76N, after 580 nm laser excitation in buffer solution, pH 6

	SRI-WT (ST method)*	SRI-WT (TT method)#	SRI-D76N (ST method)	SRI-D76N (TT method)
[NaCl] = 0.5 M				
α_{th1} ($\tau_{pr} < 10$ ns)§	0.70 ± 0.05	0.70 ± 0.05	0.64 ± 0.05	0.68 ± 0.01
$\Delta V_{r,1}$ (mL/mol)	2.2 ± 0.1	2.5 ± 0.5	0.76 ± 0.24	0.61 ± 0.06
Φ_{610} (lower limit)¶	0.33 ± 0.05	0.32 ± 0.05	0.36 ± 0.05	0.35 ± 0.01
$\Delta V_{R,1}$ (mL/mol)‖	5.5 ± 0.3	6.3 ± 1.3	1.5 ± 0.5	1.2 ± 0.1
α_{th2} (1.5 μs $< \tau_{610} <$ 2.5 μs)	—	—	0.05 ± 0.05	—
$\Delta V_{r,2}$ (mL/mol)	—	—	2 ± 1	—
[NaCl] = 0.25 M				
α_{th1} ($\tau_{pr} < 10$ ns)	0.7 ± 0.1	0.7 ± 0.1	0.60 ± 0.05	0.67 ± 0.04
$\Delta V_{r,1}$ (mL/mol)	3.0 ± 1.5	2.2 ± 0.4	1.3 ± 0.4	0.9 ± 0.1
Φ_{610} (lower limit)	0.4 ± 0.1	0.3 ± 0.1	0.43 ± 0.05	0.36 ± 0.04
$\Delta V_{R,1}$ (mL/mol)	7.5 ± 4	5.5 ± 1	2.6 ± 0.8	1.8 ± 0.2
α_{th2} ($\tau_{610} \approx 2$ μs)	—	—	0.09 ± 0.03	—
$\Delta V_{r,2}$ (mL/mol)	—	—	1.0 ± 0.5	—

*For the ST method, T = 3–20°C for 0.25 M NaCl ($c_p\rho/\beta$ = 69–12 kJ/mL) and 2–15°C for 0.5 M NaCl ($c_p\rho/\beta$ = 52–14.5 kJ/mL).
#For the TT method, $T_{\beta=0}$ = 0°C (0.25 M NaCl), and −3.5°C (0.5 M NaCl).
§α_{thi} (= q_i/E_λ) and $\Delta V_{r,i}$ derived by applying Eq. 1 (ST method) or Eq. 2 (TT method).
¶The lower limit for Φ_{610} is derived from Eq. 4.
‖The value of $\Delta V_{R,1}$ (structural volume change per mol of phototransformed molecules) is calculated by means of the relation $\Delta V_{r,1} = \Phi_{610}\Delta V_{R,1}$, using the flash photolysis values Φ_{610} = 0.4 for SRI-WT and 0.5 for SRI-D76N.

step from the E_{0-0} level is obtained. In other words, E_{S610} is 24% lower than the E_{0-0} value (187 kJ/mol). For SRI-D76N, the same value is obtained, indicating that the mutation at Asp[76] to asparagine does not affect the energy level of the first transient.

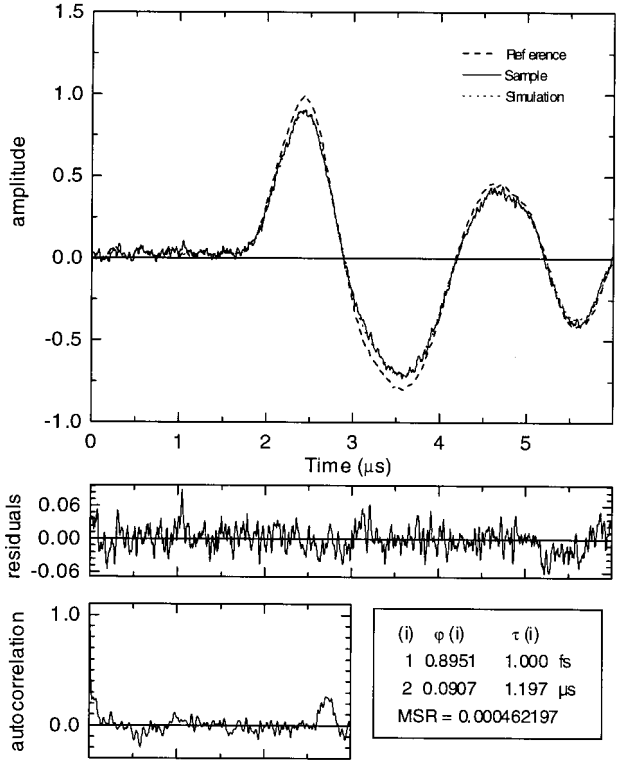

FIGURE 5 LIOAS waveform for SRI-D76N at 18°C; the reference signal has the largest amplitude. Included are the residuals distribution and the autocorrelation function after fitting by deconvolution. The curve obtained after deconvolution is superimposed to the sample waveform. The value of τ_{pr} has no physical meaning, it includes all prompt processes. τ_{610} = 1.2 μs.

The first step, i.e., the energy released upon formation of the first transient, is thus much smaller than the corresponding process in BR where a loss of ~70% of absorbed energy per phototransformed mole was determined (Schulenberg et al., 1994; Zhang and Mauzerall, 1996), although the chemical process (all-*trans* to 13-*cis* photoisomerization of the retinal chromophore) is identical in both proteins. An even smaller gap of only 7% between the 0−0 band and the first intermediate has recently been determined for the batho product of rhodopsin (Strassburger et al., 1997) which comprises, however, the 11-*cis* to all-*trans* photoisomerization as the photochemical primary process.

The specific molecular basis of the structural volume changes in the early step of the phototransformation in each of the retinal proteins is not yet understood, but it should be related to the movements of amino acid residues or of water molecules inside the retinal cavity, affording changes in specific interactions between the isomerized chromophore and its microenvironment. Contributions resulting from electrostriction effects are expected to be negligible, because in no case the Schiff base releases the proton in this

TABLE 4 LIOAS data for SRI-WT and SRI-D76N at two pH values

	SRI-WT		SRI-D76N	
	pH 6	pH 7	pH 6	pH 7.2
[NaCl] = 0.5 M				
α_{th1} ($\tau_{pr} < 10$ ns)	0.77 ± 0.05	0.79 ± 0.05	0.70 ± 0.05	0.71 ± 0.06
$\Delta V_{r,1}$ (mL/mol)	1.8 ± 0.8	2.8 ± 0.4	1.1 ± 0.1	1.8 ± 0.1
Φ_{610} (lower limit)	0.28 ± 0.05	0.26 ± 0.05	0.36 ± 0.05	0.35 ± 0.06
$\Delta V_{R,1}$ (mL/mol)	4.5 ± 2	7.0 ± 1	2.2 ± 0.2	3.6 ± 0.2

λ_{exc} = 532 nm, ST method. Evaluation of the data as described in Table 3.

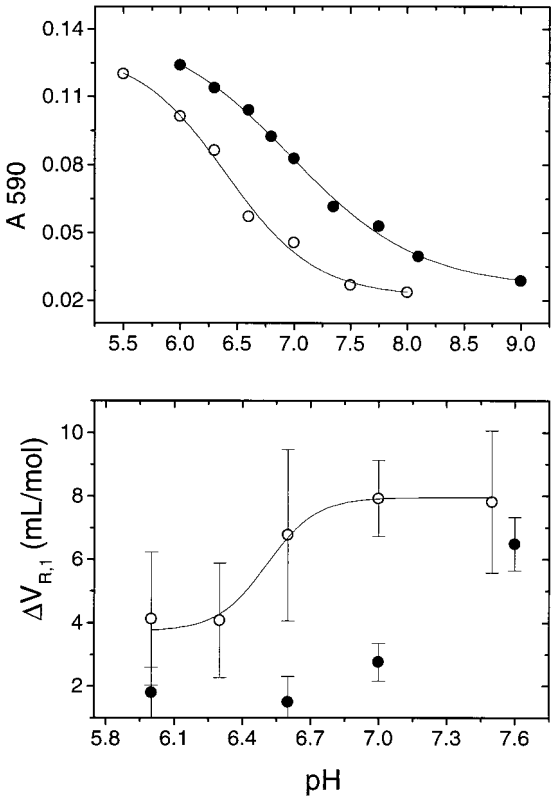

FIGURE 6 pH dependence of 590 nm absorbance (*top*) and $\Delta V_{R,1}$ (related to $\tau_{pr} < 10$ ns) (*bottom*) derived from LIOAS experiments, for SRI-WT (*open circles*) and for SRI-D76N (*full circles*). $\lambda_{exc} = 532$ nm for SRI-WT and 580 nm for SRI-D76N; the TT method was used. The titration curves of the absorbances were fitted on the basis of a one proton release ($pK_a = 6.4$ and 6.9 for WT and D76N mutant, respectively), whereas the titration curve of the structural volume changes shows a steeper rise indicative of a release of more than one proton. For details see text.

step, and recent studies have shown that the dipole moment of Schiff-base retinal does not appreciably change upon isomerization [$\Delta\mu = 0.2–0.4$ D, (Locknar and Peteanu, 1998)]. It is more conceivable that the expansion reflects the partial disruption of weak interactions (i.e., hydrogen bonds) between the chromophore and the adjacent amino acid residues, as has been demonstrated by measurements of the charge distribution in oriented BR samples (Drachev et al., 1978). For the corresponding step in BR (the production of the K intermediate), Zhang and Mauzerall (1996) suggested that the expansion is related to the restructuring of BR-trimer clusters, because they were able to observe the changes only in purple membranes and not in detergent, where BR is monomeric. In the case of SRI, the exact configuration of SRI in detergent is not known, and we cannot a priori exclude some contribution coming from the formation of protein clusters in the micelles. However, the low scattering of the solutions argues against significant aggregation.

For SRI-WT and for SRI-D76N, the lower limits for the quantum yield of formation of S_{610} calculated from LIOAS data are very similar, i.e., $\Phi_{610} \geq 0.3 \pm 0.04$ and $\geq 0.4 \pm 0.06$ for SRI-WT and for SRI-D76N, respectively, which agree very well with the values derived from laser flash photolysis (0.4 ± 0.05 and 0.5 ± 0.05, respectively). The similarity in the values for both proteins indicates that the formerly reported lower quantum yield of S_{373} in SRI-D76N [20% of that of the WT protein, (Rath et al., 1994)] is due to changes in subsequent steps of the photocycle, and not to a lower efficiency of the primary photochemical step. Additionally, the similarity in the values obtained by flash photolysis and by LIOAS confirms the validity of the assumptions implicit in Eqs. 3 and 4, i.e., the applicability of a simple model for the energy balance, neglecting secondary photochemistry. This appears to be particularly valid in the low energy range, which ensures the excitation of less than 1–2% of the molecules in flash photolysis and 2–3% in the LIOAS experiments.

Based on the fact that, for both SRI-WT and SRI-D76N, the value of $\Delta V_{R,1}$ increased at higher pH values, this phenomenon cannot be related to the protonation of Asp^{76}, which is missing in the mutant. It seems unlikely that the increase of $\Delta V_{R,1}$ with pH relates to the protonation of the Schiff base either, in view of the fact that excitation at 580 nm is absorbed only by the protonated Schiff base. Therefore, other residues in the retinal pocket may be involved.

The decay of S_{610} was the only step accelerated in the transducer-free preparation with respect to the transducer-linked protein [$\tau_{S610} = 90$ μs, (Bogomolni and Spudich, 1987) see Fig. 7]. For such comparison, however, one has to keep in mind that, besides presence or absence of the transducer, both samples are in different environments, i.e., either being embedded into the membrane or being solubilized by detergent. All the other steps of the photocycle appear to be slower (Table 1), as compared to $\tau_{S560} = 270$ μs and $\tau_{S373} = 750$ ms for the transducer-linked SRI-WT in membranes at 21°C and in 4 M NaCl, (Bogomolni and Spudich, 1987).

The differences in the S_{610} lifetimes for the two proteins, WT and the mutant (Table 1), arising from the differences in the activation parameters for the S_{610} decay (Table 2), indicate that the single D76N mutation induces significant changes in the structure of the cavity surrounding the chromophore. By using the ideas put forward by Beece et al. (1981) on the meaning of the activation parameters in the case of protein reactions, it can be concluded that a larger preexponential Arrhenius factor implies a more rigid environment of the region undergoing the transformation (Lindemann et al., 1993). Accordingly, the $\Delta S^{\#}$ and $\Delta H^{\#}$ values derived from the Eyring fitting indicate that a relatively small change in the value of $\Delta H^{\#}$ is compensated by a variation in $\Delta S^{\#}$, i.e., less bond breaking is necessary in SRI-D76N to reach the transition state. Thus, the activation entropy is smaller and an enthalpy-entropy compensation effect arises (Lindemann et al., 1993; Dunitz, 1995) for the $S_{610} \rightarrow S_{560}$ decay. Asp^{76} is mainly protonated at pH 6 and thus the mutation is not expected to affect the charge distribution in the vicinity of the retinal. However, it has been shown that, in SRI, the retinal pocket is very rigid and the

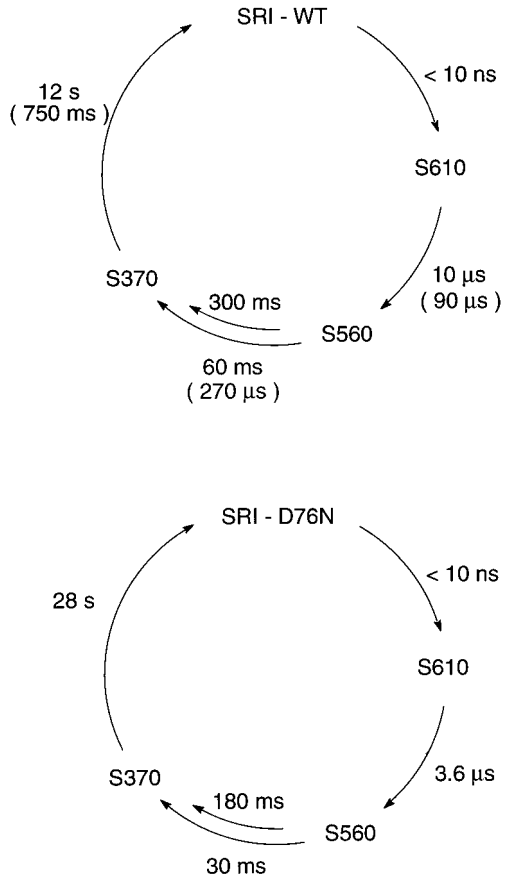

FIGURE 7 Comparison between the photocycles of detergent solubilized SRI-WT and membrane-embedded SRI-*Htr*I complex (*top*) (data in parentheses are from Bogomolni and Spudich, 1987), and the D76N mutant (*bottom*). Note that the data from this work were obtained at 6°C, whereas the literature values refer to measurements at ambient temperature and with very different preparations.

chromophore is subject to considerable steric constraints (Yan et al., 1993; Lin and Yan, 1997). It is thus conceivable that even a small change in the microenvironment surrounding the retinal results in large modifications of the steric interactions. Most probably, this also induces changes in the hydrogen bonds, which are ubiquitously involved in enthalpy-entropy compensation effects in biological systems (Dunitz, 1995; Grunwald and Comeford, 1995).

With the above considerations, it is interesting that SRI-D76N and SRI-WT show different structural volume changes upon formation of the fast intermediate, though they present similar formation quantum yields and energy levels. The larger expansion observed in SRI-WT could correspond to a more extended weakening or even disruptions of the hydrogen bonds accompanying the SRI $\rightarrow S_{610}$ step. It should be noted, however, that the activation parameters discussed above relate to the $S_{610} \rightarrow S_{560}$ process, and not to the production of S_{610}, as determined by LIOAS.

Φ_{610} appears to be similar for the two proteins (vide supra), whereas the yield of S_{373} formation is quite smaller for SRI-D76N [~50% lower than SRI-WT in our solutions and 20% of the SRI-WT in membranes (Rath et al., 1994)]. The rise of S_{373} was biexponential with rate constants k_3 (τ_3^{-1}) and k_4 (τ_4^{-1}). SRI-D76N exhibits very similar τ_3 and τ_4 values as SRI (Table 1).

In SRI-D76N, the $S_{610} \rightarrow S_{560}$ decay was also accompanied by an expansion and by a very small enthalpic change, suggesting that $\Phi_{610} \times (E_{610}/E_\lambda) \approx \Phi_{560} \times (E_{560}/E_\lambda)$ in Eq. 5.

The $S_{560} \rightarrow S_{373}$ and $S_{373} \rightarrow$ SRI processes are considerably slower in our system than in the complex SRI-*Htr*I in membranes [Table 1 and (Bogomolni and Spudich, 1987; Haupts et al., 1996)], whereas $S_{610} \rightarrow S_{560}$ is faster. Inasmuch as the slower steps include chemical reactions (deprotonation and reprotonation of the Schiff base), it is conceivable that the removal of the transducer alters these chemical events (Yan et al., 1997). In contrast, the faster step should include vibrational relaxations and reorganization of the hydrogen bond network around the retinal, which isomerizes in this step. The removal of the transducer may facilitate the conformational changes needed to reach the transition state, thus rendering this decay faster. However, the sample preparation in the detergent-solubilized material is so different from the membrane-embedded system that comparisons are not very instructive.

A. Losi was supported by the Marie Curie grant No. ERBFMBICT972377. The careful preparations of purified SRI and D76N by Kenneth Scott and the able technical assistance by Gudrun Klihm, Dagmar Lenk, and Sigrid Russell are greatly appreciated. We are indebted to Professor Kurt Schaffner for his continuous generous support. The work was partially supported by United States Public Health Service National Institutes of Health grant R01GM27750 (to JLS).

REFERENCES

Beece, D., S. F. Bowne, J. Czége, L. Eisenstein, H. Frauenfelder, D. Good, M. C. Marden, J. Marque, P. Ormos, L. Reinisch, and K. T. Yue. 1981. The effect of viscosity on the photocycle of bacteriorhodopsin. *Photochem. Photobiol.* 33:517–522.

Bensasson, R., C. R. Goldschmidt, E. J. Land, and T. G. Truscott. 1978. Laser intensity and the comparative method for determination of triplet quantum yields. *Photochem. Photobiol.* 28:277–281.

Bogomolni, R. A., and J. L. Spudich. 1987. The photochemical reactions of bacterial sensory rhodopsin-I. *Biophys. J.* 52:1071–1075.

Bogomolni, R. A., W. Stoeckenius, I. Szundi, E. Perozo, K. D. Olson, and J. L. Spudich. 1994. Removal of transducer *Htr*I allows electrogenic proton translocation by sensory rhodopsin I. *Proc. Natl. Acad. Sci. USA.* 91:10188–10192.

Borsarelli, C. D., and S. E. Braslavsky. 1997. Nature of the water structure inside the pools of reversed micelles sensed by laser-induced optoacoustic spectroscopy. *J. Phys. Chem. B.* 101:6036–6042.

Braslavsky, S. E., and G. E. Heibel. 1992. Time-resolved photothermal and photoacoustic methods applied to photoinduced processes in solution. *Chem. Rev.* 92:1381–1410.

Butt, H. J., K. Fendler, E. Bamberg, J. Tittor, and D. Oesterhelt. 1989. Aspartic acids 96 and 85 play a central role in the function of bacteriorhodopsin as a proton pump. *EMBO J.* 8:1657–1663.

Churio, M. S., K. P. Angermund, and S. E. Braslavsky. 1994. Combination of laser-induced optoacoustic spectroscopy (LIOAS) and semiempirical calculations for the determination of molecular volume changes: the photoisomerization of carbocyanines. *J. Phys. Chem.* 98:1776–1782.

Drachev, L. A., A. D. Kaulen, and V. P. Skulachev. 1978. Time resolution of the intermediate steps in the bacteriorhodopsin-linked electrogenesis. *FEBS Lett.* 87:161–167.

Dunitz, J. D. 1995. Win some, lose some: enthalpy-entropy compensation in weak intermolecular interactions. *Chem. Biol.* 2:709–712.

Gensch, T., and S. E. Braslavsky. 1997. Volume changes related to triplet formation of water soluble porphyrins. A laser-induced optoacoustic spectroscopy (LIOAS) study. *J. Phys. Chem. B.* 101:101–108.

Gensch, T., C. Viappiani, and S. E. Braslavsky. 1999. Laser-induced time-resolved optoacoustic spectroscopy in solution. *In* Encyclopedia of Spectroscopy and Spectrometry: Photoacoustic Spectrometers, J. C. Lindon, G. E. Tranter, and J. L. Holmes, editors. Academic press, London. In press.

Grunwald, E., and L. L. Comeford. 1995. Thermodynamic mechanisms for enthalpy-entropy compensation. *In* Protein-Solvent Interactions. R. B. Gregory, editor. Marcel Dekker, Inc., New York. 421–443.

Haupts, U., E. Bamberg, and D. Oesterhelt. 1996. Different modes of proton translocation by sensory rhodopsin I. *EMBO J.* 15:1834–1841.

Haupts, U., W. Eisfeld, M. Stockburger, and D. Oesterhelt. 1994. Sensory rhodopsin I photocycle intermediate SRI(380) contains 13-*cis* retinal bound via an unprotonated Schiff base. *FEBS Lett.* 356:25–29.

Hoff, W. D., K.-H. Jung, and J. L. Spudich. 1997. Molecular mechanism of photosignaling by archaeal sensory rhodopsins. *Annu. Rev. Biophys. Biomol. Struct.* 26:223–258.

Krebs, M. P., E. N. Spudich, and J. L. Spudich. 1995. Rapid high-yield purification and liposome reconstitution of polyhistidine-tagged sensory rhodopsin I. *Protein Expr. Purif.* 6:780–788.

Lin, S. L., and B. Yan. 1997. Three-dimensional model of sensory rhodopsin I reveals important restraints between the protein and the chromophore. *Protein Eng.* 10:197–206.

Lindemann, P., S. E. Braslavsky, M.-M. Cordonnier, L. H. Pratt, and K. Schaffner. 1993. Effects of bound monoclonal antibodies on the decay of the phototransformation intermediates I1,2 700 from native Avena phytochrome. *Photochem. Photobiol.* 58:417–424.

Locknar, S. A., and L. A. Peteanu. 1998. Investigation of the relationship between dipolar properties and *cis-trans* configuration in retinal polyenes: a comparative study using Stark spectroscopy and semiempirical calculations. *J. Phys. Chem. B.* 102:4240–4246.

Losi, A., and C. Viappiani. 1998. Reaction volume and rate constants for the excited-state proton transfer in aqueous solutions of naphthols. *Chem. Phys. Lett.* 289:500–506.

Malkin, S., M. S. Churio, S. Shochat, and S. E. Braslavsky. 1994. Photochemical energy storage and volume changes in the microsecond time range in bacterial photosynthesis—a laser induced optoacoustic study. *J. Photochem. Photobiol., B Biol.* 23:79–85.

Oesterhelt, D., and W. Stoeckenius. 1997. Isolation of the cell membrane of *Halobacterium halobium* and its fractionation into red and purple membrane. *In* Biomembranes. L. Packer, editor. Academic Press, San Diego. 243–254.

Olson, K. D., and J. L. Spudich. 1993. Removal of the transducer protein from sensory rhodopsin I exposes sites of proton release and uptake during the receptor photocycle. *Biophys. J.* 65:2578–2585.

Rath, P., K. D. Olson, J. L. Spudich, and K. J. Rothschild. 1994. The Schiff base counterion of bacteriorhodopsin is protonated in sensory rhodopsin I: spectroscopic and functional characterization of the mutated proteins D76N and D76A. *Biochemistry.* 33:5600–5606.

Rath, P., E. N. Spudich, D. D. Neal, J. L. Spudich, and K. Y. Rothschild. 1996. Asp^{76} is the Schiff base counterion and proton acceptor in the proton-translocating form of sensory rhodopsin I. *Biochemistry.* 35: 6690–6696.

Ruddat, A., P. Schmidt, C. Gatz, S. E. Braslavsky, W. Gärtner, and K. Schaffner. 1997. Recombinant type A and B phytochromes from potato. Transient absorption spectroscopy. *Biochemistry.* 36:103–111.

Rudzki, J. E., J. L. Goodman, and K. S. Peters. 1985. Simultaneous determination of photoreaction dynamics and energetics using pulsed, time-resolved photoacoustic calorimetry. *J. Am. Chem. Soc.* 107:7849–7854.

Rudzki-Small, J., L. J. Libertini, and E. W. Small. 1992. Analysis of photoacoustic waveforms using the nonlinear least square method. *Biophys. Chem.* 41:29–48.

Schulenberg, P., and S. E. Braslavsky. 1997. Time-resolved photothermal studies with biological supramolecular systems. *In* Progress in Photothermal and Photoacoustic Science and Technology. 3. Life and Earth Sciences. A. Mandelis and P. Hess, editors. SPIE, Bellingham, WA. 58–81.

Schulenberg, P., M. Rohr, W. Gärtner, and S. E. Braslavsky. 1994. Photoinduced volume changes associated with the early transformations of bacteriorhodopsin: a laser-induced optoacoustic spectroscopy study. *Biophys. J.* 66:838–843.

Spudich, E. N., and J. L. Spudich. 1993. The photochemical reactions of sensory rhodopsin I are altered by its transducer. *J. Biol. Chem.* 268: 16095–16097.

Spudich, J. L., and R. A. Bogomolni. 1984. The mechanism of colour discrimination by a bacterial sensory rhodopsin. *Nature.* 312:509–513.

Strassburger, J. M., W. Gärtner, and S. E. Braslavsky. 1997. Volume and enthalpy changes after photoexcitation of bovine rhodopsin: laser-induced optoacoustic studies. *Biophys. J.* 72:2294–2303.

Tittor, J., and D. Oesterhelt. 1990. The quantum yield of bacteriorhodopsin. *FEBS Lett.* 263:269–273.

van Brederode, M. E., T. Gensch, W. D. Hoff, K. J. Hellingwerf, and S. E. Braslavsky. 1995. Photoinduced volume change and energy storage associated with the early transformations of the photoactive yellow protein from *Ectothiorhodospira halophila. Biophys. J.* 68:1101–1109.

Yan, B., E. N. Spudich, M. Sheves, G. Steinberg, and J. L. Spudich. 1997. Complexation of the signal transducing protein *Htr*I to sensory rhodopsin I and its effect on thermodynamics of signaling state deactivation. *J. Phys. Chem. B.* 101:109–113.

Yan, B., A. Xie, G. U. Nienhaus, Y. Katsuta, and J. L. Spudich. 1993. Steric constraints in the retinal binding pocket of sensory rhodopsin-I. *Biochemistry.* 32:10224–10232.

Yao, V. J. and J. L. Spudich. 1992. Primary structure of an archaebacterial transducer, a methyl-accepting protein associated with sensory rhodopsin I. *Proc. Natl. Acad. Sci. USA.* 89:11915–11919.

Zhang, H. and D. Mauzerall. 1996. Volume and enthalpy changes in the early steps of bacteriorhodopsin photocycle studied by time-resolved photoacoustics. *Biophys. J.* 71:381–388.